Journal of Zhejiang University-SCIENCE A (Applied Physics & Engineering)
ISSN 1673-565X (Print); ISSN 1862-1775 (Online)
www.zju.edu.cn/jzus; www.springerlink.com
E-mail: jzus@zju.edu.cn

Pseudo-dynamic testing of a fabricated composite frame with steel plate shear walls*

Zheng-gang CAO[1,2], Peng DU[†‡1,2], Feng FAN[1,2], Zhe-ming CHEN[3]

([1]*Key Lab of Structures Dynamic Behavior and Control of the Ministry of Education, Harbin Institute of Technology, Harbin 150090, China*)

([2]*School of Civil Engineering, Harbin Institute of Technology, Harbin 150090, China*)

([3]*Shanghai Municipal Engineering Design Institute (Group) Co. Ltd., Shanghai 200092, China*)

[†]E-mail: pengdu5219@hotmail.com

Received Jan. 16, 2016; Revision accepted Oct. 7, 2016; Crosschecked May 8, 2017

Abstract: A pseudo-dynamic testing program was generated on a fabricated composite frame with steel plate shear walls (SPSWs) to study its seismic performance. The specimen was a three-storey single-bay frame, which was composed of H-section steel columns and composite beams, and was assembled by bolted height-adjustable steel beam-to-column connections (BHA connections). Beam-only-connected SPSWs were selected as lateral load resisting members. The specimen was subjected to four ground motions of progressively increasing intensity. The results showed that: (1) beam-only-connected SPSWs provided sufficient lateral load resistance, lateral stiffness, and energy dissipation capacity to the fabricated frame via the tension field action developed in their infill panels; (2) the fabricated frame, assembled by BHA connections, exhibited substantial redundancy and good ductility; (3) an undesirable failure mode of the fabricated frame, in huge earthquakes, included severe cracking in composite beams and block shear failure in SPSWs' connections; (4) the inter-storey shear force distribution determined by ASCE/SEI 7-10 was verified with experimental data.

Key words: Fabricated frame; Composite beam; Steel plate shear walls; Pseudo-dynamic test
http://dx.doi.org/10.1631/jzus.A1600022 **CLC number:** TU317

1 Introduction

As all the structural members are manufactured in workshops and fast assembled by connections on site, fabricated construction technology can speed up the whole construction process and improve the quality of structures. Therefore, various conventional structural members and connections have been modified to meet the requirements of the fabricated construction process. Take beam-to-column connections for instance. Different hybrid-steel concrete connections for precast concrete beams using H-steel segments or thick steel plates were proposed to simplify the assembling of composite frames (Kulkarni *et al*., 2008; Li *et al*., 2009; Yang *et al*., 2010). Based on the hybrid connection concept mentioned above, Liu *et al*. (2013) replaced the tensional rebar at the bottom of concrete beams with a steel strip, welded with beam end steel connectors, to take advantage of both the high tensile strength of steel and high compressive strength of concrete, and two rows of studs were welded to the steel strip to provide the bond between steel and concrete (Fig. 1a). H-steel segments were used as steel connectors on both ends of the proposed composite beams. Compared with the conventional concrete beam (Fig. 1b), this composite beam construction not only has a higher stiffness and load-carrying capacity, but also has a simple connection with the steel columns. To minimize the negative

‡ Corresponding author

* Project supported by the National Natural Science Foundation of China (No. 51378147)

ORCID: Zheng-gang CAO, http://orcid.org/0000-0003-4764-288X; Peng DU, http://orcid.org/0000-0003-2646-9029

effect of manufacturing deviation on the assembling of structures, Cao *et al*. (2015) proposed bolted height-adjustable steel beam-to-column connections (BHA connections). As shown in Fig. 2a, a BHA connection is composed of a T-shaped connector (Fig. 2b), an L-shaped connector with ellipse-type blot holes (Fig. 2c), and several bearing-type high-strength bolts. BHA connections can adapt to a small change of the H-shaped steel beam height by adjusting the location of L-shaped connectors.

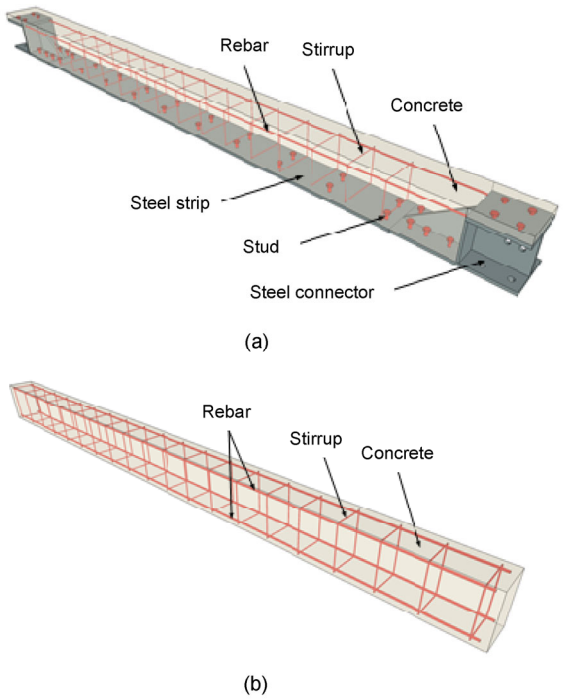

Fig. 1 Schematic diagram of composite beams and concrete beams

(a) Composite beams with steel connectors; (b) Concrete beams

For lateral load resisting systems, steel plate shear walls (SPSWs) have been considered as viable members, because they can cost-effectively satisfy the strength, lateral stiffness, and ductility requirements of buildings in high seismic zones (Driver *et al*., 1998; Lubell *et al*., 2000; Lin *et al*., 2010). A typical SPSW consists of a steel infill panel and its boundary frame members. Unstiffened infill panels will buckle under a very small shear force and resist lateral load via a series of inclined tension strips which are anchored on boundary members (Thorburn *et al*., 1983). However, the boundary members and their moment-resisting beam-to-column connections may fail prematurely owing to the extra internal force in boundary members induced by the tension strip actions. This will lead to obvious residual deformations and costly repair. Xue and Lu (1994) proposed SPSWs only connected with boundary beams to reduce the negative effect of tension strips on columns. Their analytical results showed that the early failure of columns could be prevented by this SPSW construction. Guo *et al*. (2011) investigated the hysteretic behavior of beam-only-connected SPSWs via quasi-static experiments, and their results showed that this kind of SPSWs could exhibit good ductility and excellent energy dissipation capacity. As an innovative solution, SPSWs have been combined with post-tensioned beam-to-column connections to realize the self-centering of the deformed frames, and the quasi-static test results demonstrated that the system possessed self-centering capacity and at the same time could maintain the high initial stiffness, strength, energy dissipation, and ductility provided by infill panels (Clayton *et al*., 2012a; 2012b; Dowden *et al*., 2012).

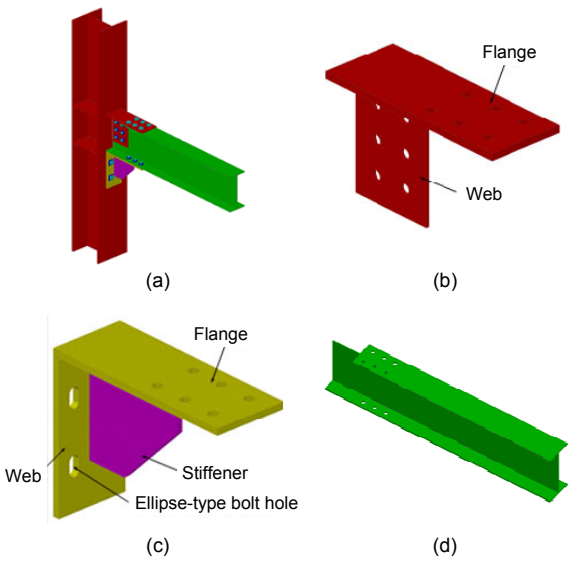

Fig. 2 BHA connections

(a) Assembly drawing; (b) T-shaped connector; (c) L-shaped connector; (d) Beam end with top flange partial removed

Most existing research focused on the behavior of the steel frame with conventional SPSWs. For example, two 8-m tall and 4-m wide, two-storey

steel plate shear walls, connected with both steel beams and columns, were tested using pseudo-dynamic test technology to study the seismic response of SPSWs (Qu *et al*., 2008; Lin *et al*., 2010). However, there has been limited research on the seismic response of the fabricated composite frame with beam-only-connected SPSWs under real ground motions. To address this issue, a pseudo-dynamic experiment program was conducted to test a three-storey single-bay fabricated frame having H-section steel columns, composite beams, and BHA connections. Beam-only-connected SPSWs were used as lateral load resisting members in the specimen. The testing program investigated the seismic performance of the proposed structural system under four progressively increasing ground motions. This paper summarizes the test procedure, experimental observations, and the structural response of the specimen.

2 Test program

2.1 Specimen design

The prototype of the specimen was an existing three-storey residential steel frame, including two beam-only-connected SPSW frames in its transverse direction (Fig. 3a). The test frame was 9000 mm high (3000 mm at each storey) and 4000 mm wide, as measured between boundary frame member centerlines (Fig. 3b). The test was conducted in the Structural and Earthquake-resistant Testing Center of the School of Civil Engineering at Harbin Institute of Technology, China. Based on the capacity of hydraulic actuators and the anchor hole arrangement on the reaction wall and strong floor, the test prototype frame was scaled with a geometrical scale factor of 1:2, and the scaled storey height and width were 1500 mm and 2000 mm, respectively. The member sections of the prototype are listed in Table 1. The scaled P1 and B1 sections in the specimen are also shown in this table. To study the performance of precast composite beams in the proposed fabricated structural system, the steel beams in the specimen were replaced by the composite beam with steel connectors as in Fig. 1a, whose section was proportioned from the scaled B1 section based on the equivalent capacity principle. The details of the designed composite beam are shown in Figs. 4 and 5. Fishplates were embedded in composite beams to connect with beam-only-connected SPSWs (Fig. 5a). According to the Chinese specification for seismic test of buildings JGJ/T 101-2015 (MOHURD, 2015), the scaled model should meet the requirement of dynamical similarity. To verify the dynamical similarity of this test, the natural periods of the prototype building and the specimen were analyzed using commercial software SAP2000. The calculated similarity factor for the first natural period was 1.6:1, which was close to the specification requirement of $\sqrt{2}$:1.

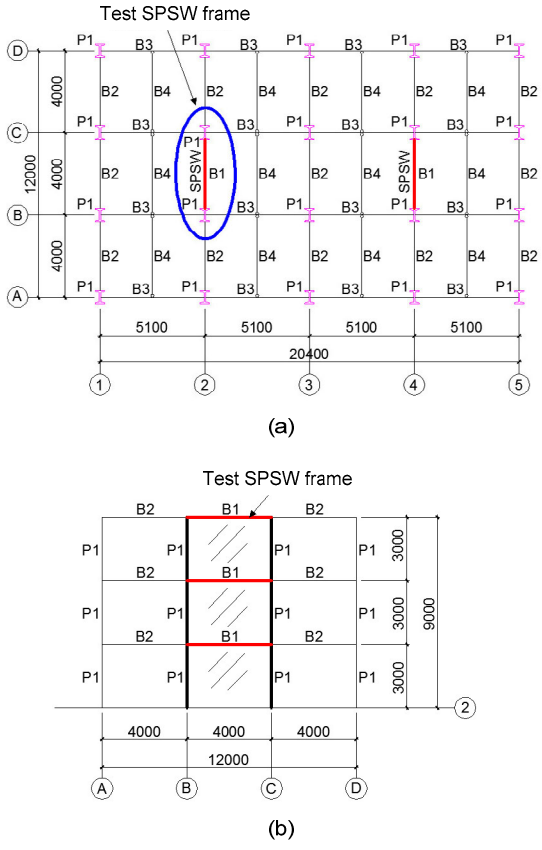

Fig. 3 Schematic drawing of prototype (unit: mm)
(a) Floor plan; (b) Elevation view of the test SPSW frame

Table 1 Member sections of prototype and specimen (unit: mm)

Section No.	Prototype	Specimen
P1	HW200×200×12×16	HW100×100×6×8
B1	HN160×80×6×10	HN80×40×3×5
B2	HN150×75×5×7	–
B3	HN200×100×5.5×8	–
B4	HN125×60×6×8	–

BHA connections were implemented in the specimen to join H-section steel columns and composite beams together in the lab. The capacity design method was applied to check the strength of BHA connections, and the details of the designed BHA connections are illustrated in Fig. 6.

The steel infill panels of beam-only-connected SPSWs were sized based on the recommendations provided by Guo *et al*. (2011):

$$K_0 = \frac{E_s t}{1/(L/H)^3 + 2(1+v_s)\cdot k/(L/H)}, \quad (1)$$

$$V_u = [0.23\ln(L/H) - 0.13\ln\lambda + 1.22]\cdot f_v L t, \quad (2)$$

where K_0 is the elastic stiffness of beam-only-connected SPSWs, E_s is Young's modulus of steel, t denotes the thickness of infill panels, v_s is Poisson's ratio of steel, k is the correction coefficient considering non-uniform shear stress distribution on the cross-section, L and H are the length and height of infill panels, respectively, V_u is the ultimate load-carrying capacity of beam-only-connected SPSWs, λ denotes the height-to-thickness ratio of the infill panel, and f_v denotes the shear yield stress of steel. The selected infill panel was 2 mm thick for each storey, and its machining dimensions are shown in Fig. 7.

2.2 Test setup and measuring instrument arrangement

The specimen was attached to the strong floor via the reaction beam (Fig. 8). Pseudo-dynamic

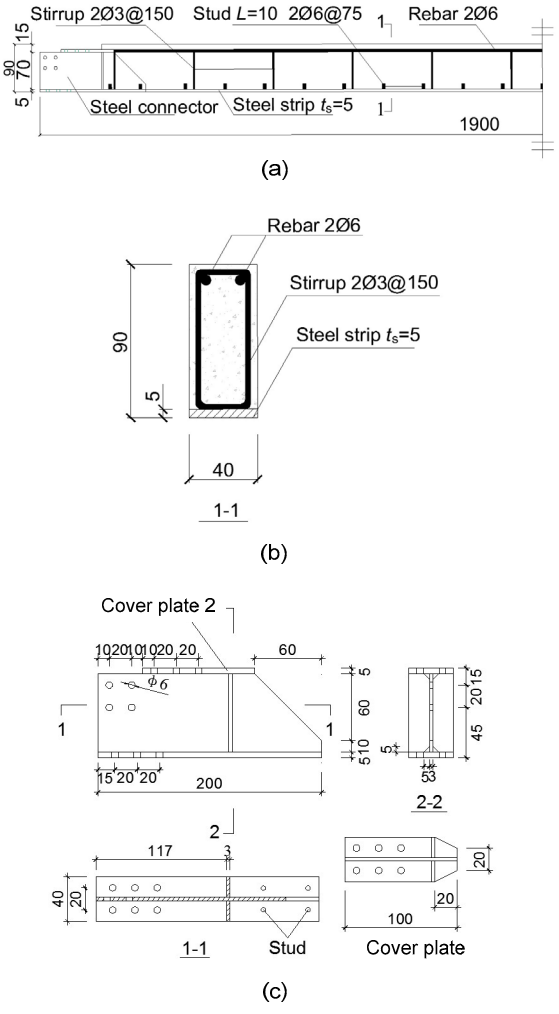

Fig. 4 Details of composite beams (unit: mm)
(a) Composite beam; (b) Composite beam section; (c) Steel connector

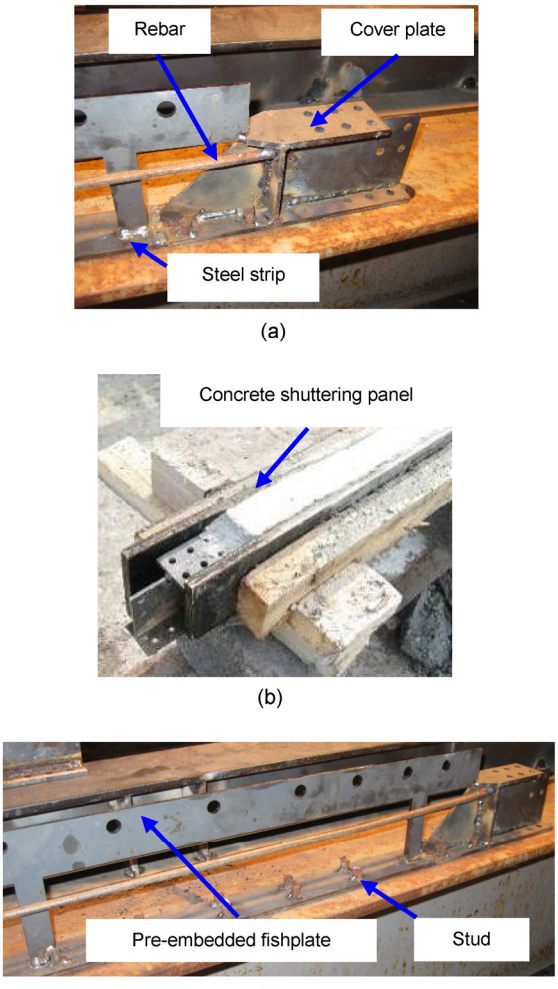

Fig. 5 Processing of composite beams
(a) Steel beam end; (b) Casting of concrete; (c) Fishplate

loads were applied by the in-plane servo-controlled hydraulic actuators mounted between the specimen and the reaction wall. Based on the pushover analysis result of the specimen, one 100-t hydraulic actuator was employed for each storey. To prevent out-of-plane movement of the specimen, a lateral bracing system was installed at the top beam (Fig. 8). To obtain the stress distribution in critical regions, strain gauges were bonded to boundary frame member ends, BHA connection connectors, and infill panels. The displacement responses of three storeys were recorded by the linearly variable displacement transformers (LVDTs) placed on beam ends. The load applied to each storey was measured by a load cell mounted between the specimen and a hydraulic actuator. A dial indicator was placed on the reaction beam end to monitor the possible slippage of the specimen.

2.3 Material properties

The steel and concrete used in the specimen were Chinese Grade Q235B and C40, respectively. The average coupon test results of the steel used in beams, columns, BHA connection connectors, and infill panels are shown in Table 2, all of which were sampled and tested according to the Chinese Standard GB/T 2975-1998 (MOHURD, 1999) and GB/T 228.1-2010 (MOHURD, 2011). The tested compressive strength and elastic modulus of the concrete in composite beams were 44.5 MPa and 28 GPa, respectively.

2.4 Loading protocol

To study the performance of the proposed structural system in different seismic intensities, the specimen was first tested under three sets of pseudo-dynamic loads which were obtained based on the EL

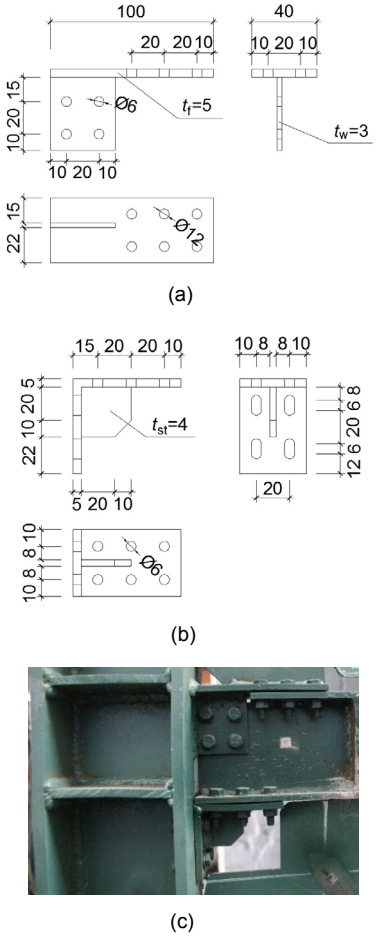

Fig. 6 Details of BHA connections (unit: mm)
(a) T-shaped connector; (b) L-shaped connector; (c) Assembled BHA connection

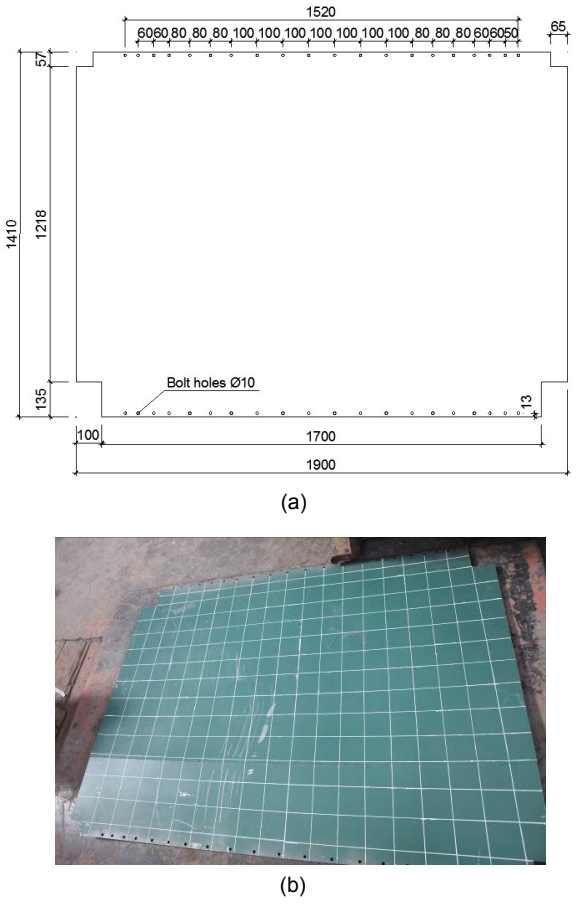

Fig. 7 Infill panel of beam-only-connected steel plate shear walls (unit: mm)
(a) Details of infill panels; (b) Infill panel prior to installation

Centro earthquake record (1940). According to the Chinese seismic design code GB50011-2010 (MOHURD, 2010), the earthquake record was scaled with the peak ground acceleration (PGA), having a 2% probability of exceedance in 50 years, in three top aseismic design intensities. For the purpose of discussion, the three intensity cases are denoted as C1, C2, and C3. On the other hand, based on the geometric scale factor mentioned previously, the calculated time scale factor was $\sqrt{2}:1$ (JGJ/T 101-2015) (MOHURD, 2015), by which the interval of the ground motion record was reduced from 0.005 s to 0.0035 s. As the PGA of the ground motion was reached in the first four seconds, only the initial 4.2 s of the scaled ground motion record was applied in the first three loading cases to save time. The PGA and duration of the first three loading cases are shown in Table 3. To investigate the behavior of the specimen in huge earthquakes, 10.5 s of the EL Centro earthquake record (1940), whose PGA was scaled up to 0.9*g*, was applied after the first three loading cases (denoted as C4). Both the original and the continued scaled ground acceleration records are shown in Fig. 9.

3 Experimental results and discussion

3.1 Experimental observations

During the C1 loading case, the specimen stayed in the elastic stage and no obvious phenomenon was observed (Fig. 10a). The beam-only-connected SPSW at the first storey buckled with a loud noise in the C2 loading case, and a slight out-of-plane deformation of the infill panel was detected at the same time (Fig. 10b). In the C3 loading case, all the

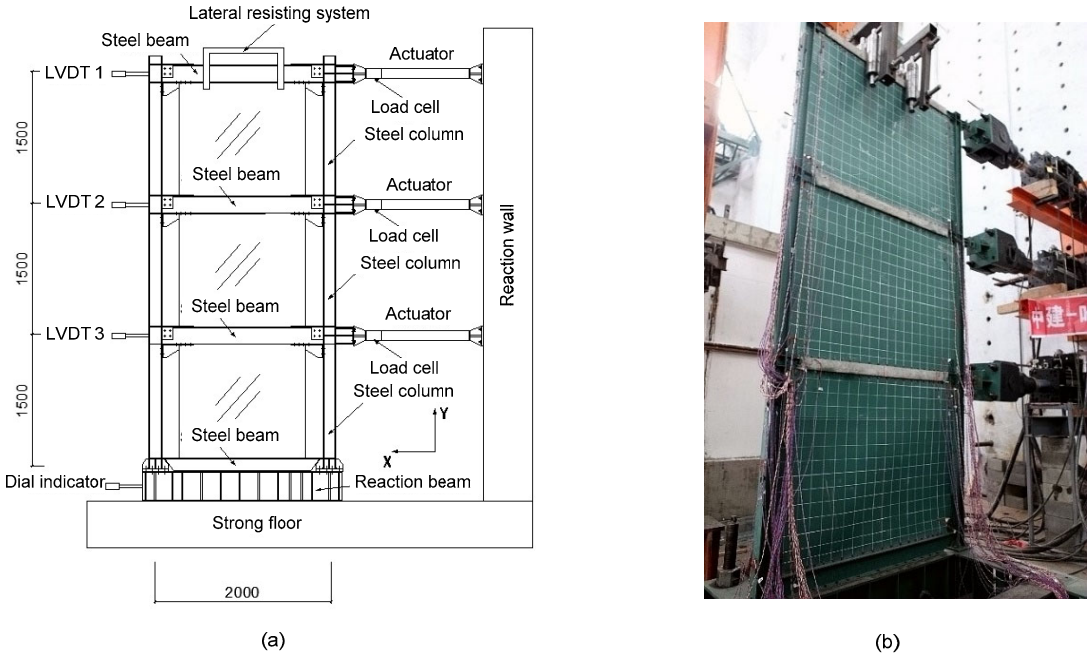

Fig. 8 Test setup (unit: mm)
(a) Schematic of test setup; (b) Specimen prior to test

Table 2 Average coupon test results of steel

Designed thickness (mm)	Actual thickness (mm)	Yielding strength (MPa)	Ultimate strength (MPa)	Elastic modulus (GPa)	Poisson's ratio
2	1.90	200	315	170	0.30
4	3.86	231	310	223	0.29
6	5.89	215	311	203	0.29
8	7.88	229	321	213	0.31

SPSWs were significantly buckled, and an obvious diagonal tensional field was found in the bottom infill panel (Fig. 10c). Therefore, the lateral loads began to be resisted by the tension field action of infill panels. The concrete on the first storey composite beam ends was also cracked (Fig. 10d), which meant that plastic hinges were first formed on composite beam ends, instead of on steel column ends. This was in accordance with the design assumption recommended by ANSI/AISC 341-10 (AISC, 2010).

When the specimen was loaded in the C4 loading case, crossed diagonal tensional strips were developed more obviously in each infill panel (Figs. 11a–11c). The connections between infill panels and fishplates failed due to the block shear of bolt connections (Fig. 11d), most of which occurred in low-rising storeys. Due to the additional tension force induced by the diagonal tension actions in infill panels and the insufficient transverse shear-resisting capacity in composite beams, horizontal cracks were observed on each beam end and progressed toward to the middle of composite beams (Fig. 11e). It was an undesirable failure mode and indicated that composite beams should be well designed with more transverse load-resisting capacity to anchor the diagonal tensional strips of infill panels. BHA connections stayed in the elastic stage and worked as rigid connections during the four loading cases. No significant slippage of connectors was observed (Fig. 11f).

Table 3 Peak ground acceleration (PGA) and duration of the four loading cases

Case	PGA	Duration (s)	Case	PGA	Duration (s)
C1	0.22*g*	4.2	C3	0.62*g*	4.2
C2	0.4*g*	4.2	C4	0.9*g*	10.5

g is the acceleration due to gravity

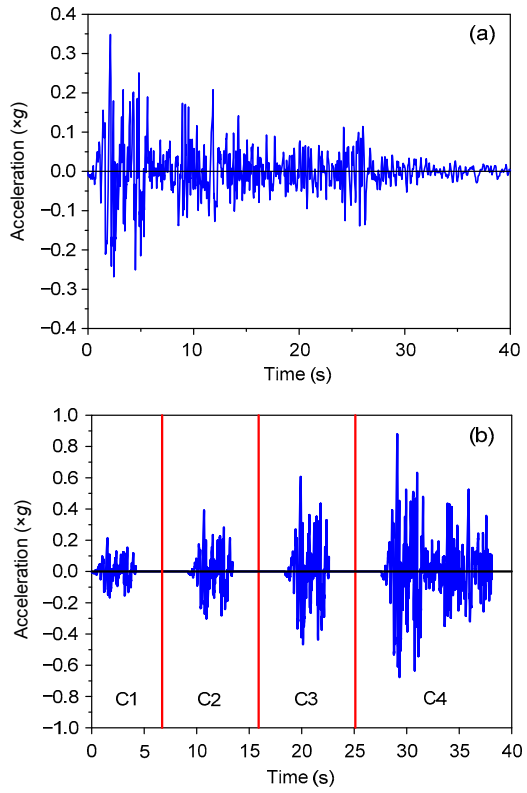

Fig. 9 Ground acceleration record of the EL Centro earthquake (1940)
(a) Original ground acceleration; (b) Continued scaled ground acceleration

3.2 Displacement response

The displacement response and the maximum inter-storey drift distribution of the specimen at floor

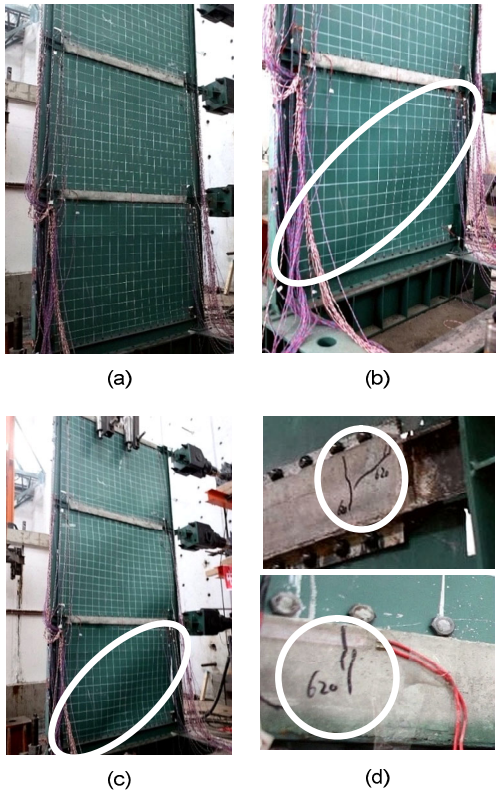

Fig. 10 Experimental observations during the first three loading cases
(a) Specimen in the elastic stage (C1); (b) Infill panel buckling (C2); (c) Infill panel buckling (C3); (d) Cracks at composite beam ends (C3)

levels are shown in Figs. 12 and 13, respectively. During the four loading cases, all the storeys in the specimen had a similar displacement waveform, and their inter-storey drift amplitudes decreased from bottom to top (Fig. 12), which indicated that the proposed fabricated composite frame could act in a shear-dominated low-order mode of vibration in earthquakes. As shown in Fig. 13, the peak storey drift ratio of the specimen in the first three loading cases ranged from 0.17% to 0.91%, and the largest drift was always found in the first storey. For the huge earthquake case (the C4 loading case), the maximum storey drift ratio reached 1.85% in the first storey (Fig. 13), and the maximum roof displacement in this case was 46.01 mm corresponding to a global drift ratio (roof displacement divided by building height) of 1.02% (Fig. 12d). All the inter-storey drifts in the four loading cases were less than 2%, which could meet the stiffness requirement of the Chinese design specification for SPSWs (JGJ/T 380-2015) (MOHURD, 2016). It can be seen from Fig. 13 that the change of inter-storey drifts along the three storeys of the specimen remained linear in

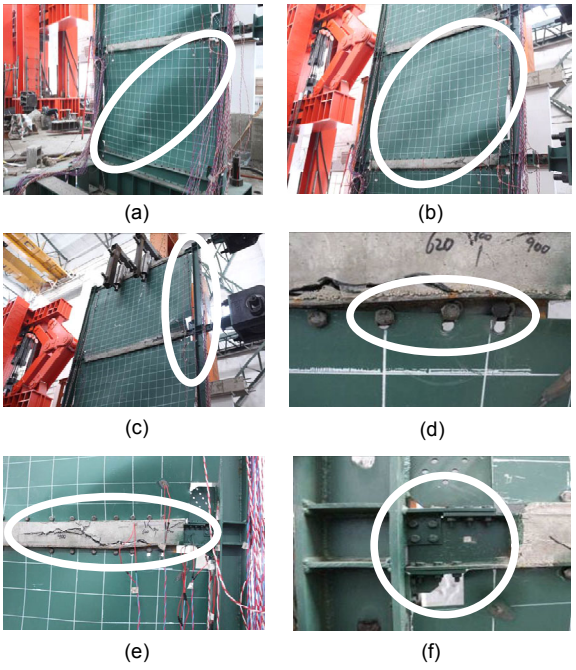

Fig. 11 Experimental observations in the C4 loading case
(a) First-storey infill panel buckling; (b) Second-storey infill panel buckling; (c) Third-storey infill panel buckling; (d) Block shear failure of bolt connections; (e) Horizontal cracks in composite beams; (f) BHA connections

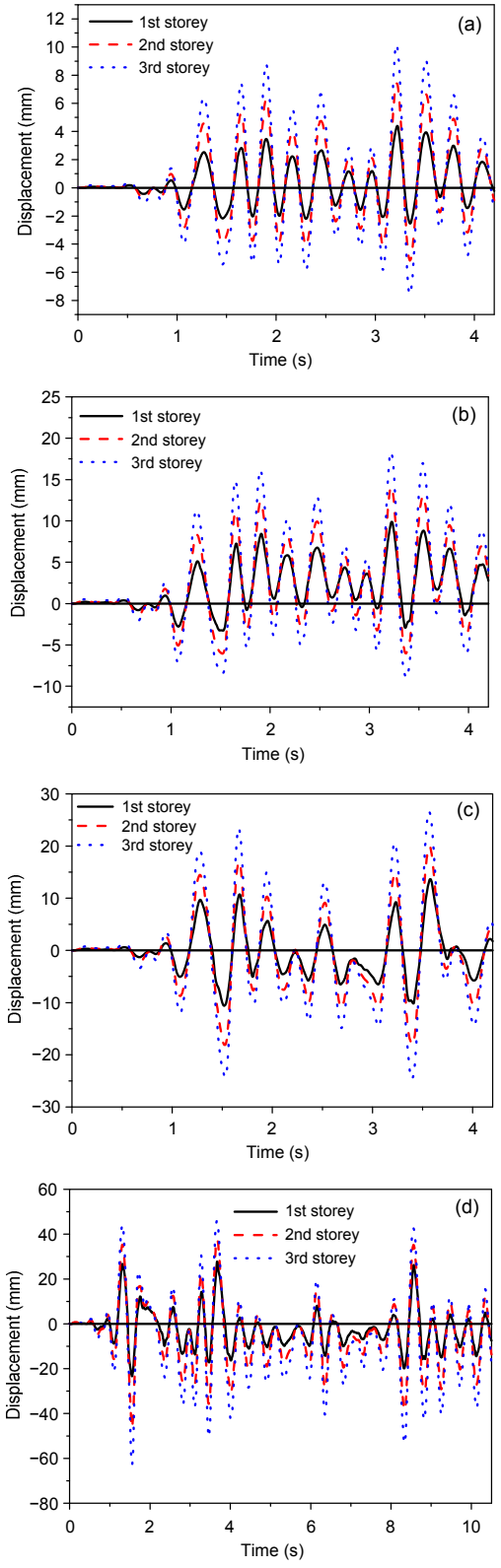

Fig. 12 Storey displacement time history responses
(a) C1 loading case; (b) C2 loading case; (c) C3 loading case; (d) C4 loading case

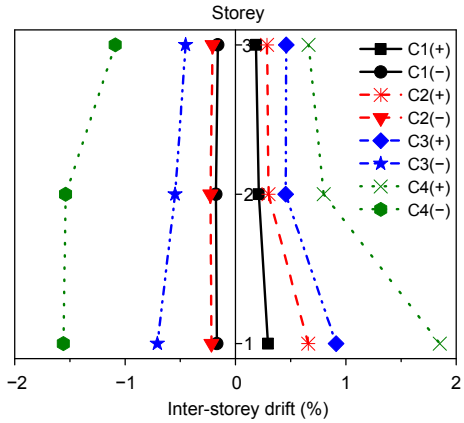

Fig. 13 Maximum inter-storey drift at floor levels

the C1 loading level, while the inter-storey drift of the first storey increased faster than others in subsequent loading levels and the drift distribution became nonlinear. It meant that the first storey was the soft-storey for the prototype building and needed to be strengthened with a thicker infill panel.

3.3 Hysteretic properties

Fig. 14 depicts the relationship between the inter-storey drift and the storey shear of the specimen in the four loading levels. For illustration purposes, only the initial 4.2 s of hysteretic response in the C4 loading case is shown in Fig. 14, and the complete hysteretic curves in the C4 loading case are provided at each storey in Fig. 15. The test results confirmed that the specimen experienced nonlinear responses during the four loading cases, and it appeared that the nonlinear responses were more significant with the increase of PGA. In addition, the nonlinear responses in the first storey were more obvious than those in other storeys, which was in accordance with the inter-storey drift responses mentioned above and demonstrated once more that the first storey was the critical storey of the specimen. Although the hysteretic curves of the specimen were pinched due to the early buckling of SPSWs, the specimen exhibited stable force-displacement behaviors during the whole test process.

As shown in Fig. 15, the first storey of the specimen could undergo plastic rotation of 0.0185 rad in the C4 loading case, which was close to the minimum rotation requirement for the highly ductile members (0.02 rad) in ANSI/AISC 341-10 (AISC, 2010). In addition, it is worth noting that no significant

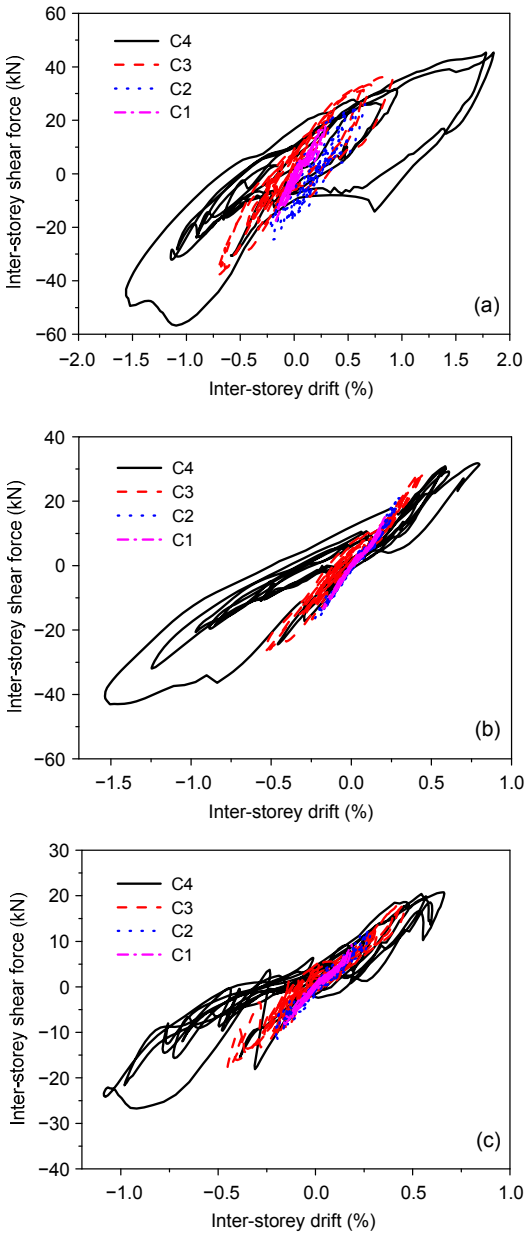

Fig. 14 Hysteretic curves at each floor
(a) First storey; (b) Second storey; (c) Third storey

strength degradation was detected during the whole loading process (Fig. 15), and the actual ultimate plastic rotation of the specimen should be larger than the aforementioned value (0.0185 rad). Therefore, it can be concluded that the specimen possessed good ductility during the test.

3.4 Energy dissipation

Figs. 16 and 17 present the accumulated dissipated energy of the specimen in the four loading

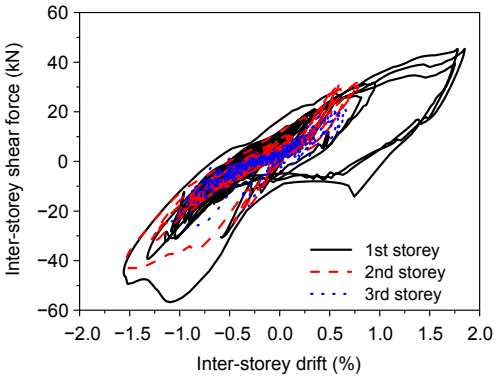

Fig. 15 Hysteretic curves at each floor in the C4 loading case

cases. As most structural members stayed in the elastic stage during the C1 loading case, the energy dissipation in this case was negligible. With the yielding of diagonal tension strips developed in beam-only-connected SPSWs and the cracking of composite beam ends, the energy dissipation gradually became pronounced in subsequent loading cases. As shown in Fig. 17, the energy dissipated in the first storey was larger than those in other storeys, because more storey shear force and inter-storey drift were induced in this storey.

3.5 Inter-storey shear force distribution

According to ASCE/SEI 7-10 (ASCE, 2010), the lateral seismic force induced at any storey can be determined using the vertical distribution factor C_{vx}, which is calculated by

$$C_{vx}=\frac{w_x h_x^k}{\sum_{i=1}^{n} w_i h_i^k}, \tag{3}$$

where w_i (or w_x) is the portion of the total effective seismic weight of the specimen located or assigned to level i (or x), h_i (or h_x) is the height from the base to level i (or x), and k is an exponent related to the structure period and is taken as 1.05 in this study. The C_{vx} calculated for the specimen is shown in Fig. 18. The inter-storey shear force distribution along the three storeys of the specimen, determined based on C_{vx} and experimental data, is shown in Fig. 19. It proved that the vertical distribution determining method of seismic force, recommended by ASCE/SEI 7-10 (ASCE, 2010), could properly predict the inter-storey shear force at each storey.

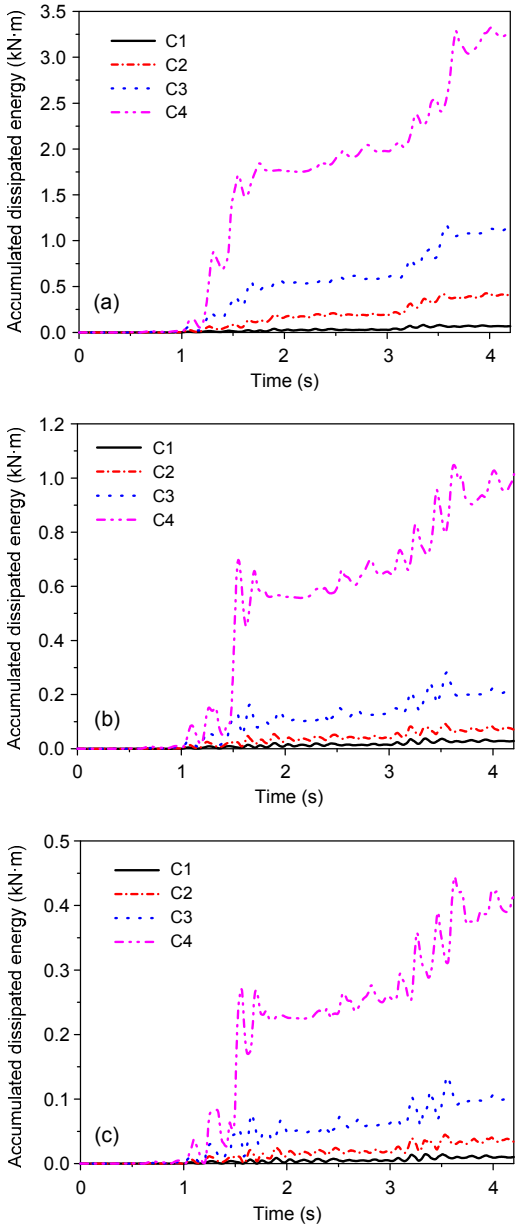

Fig. 16 Accumulated dissipated energy at each floor
(a) First storey; (b) Second storey; (c) Third storey

4 Conclusions

A scaled three-storey single-bay fabricated composite frame with steel plate shear walls was designed and tested under pseudo-dynamic loads to

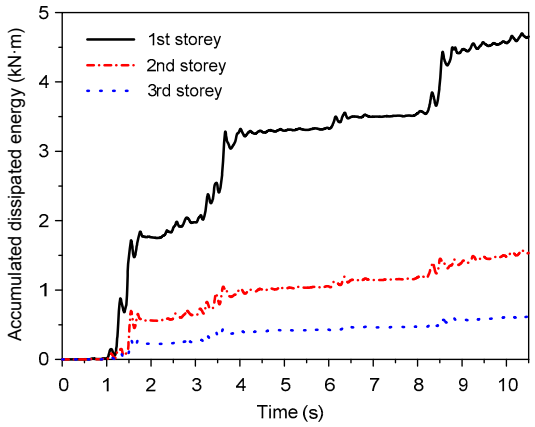

Fig. 17 Accumulated dissipated energy at each floor in the C4 loading case

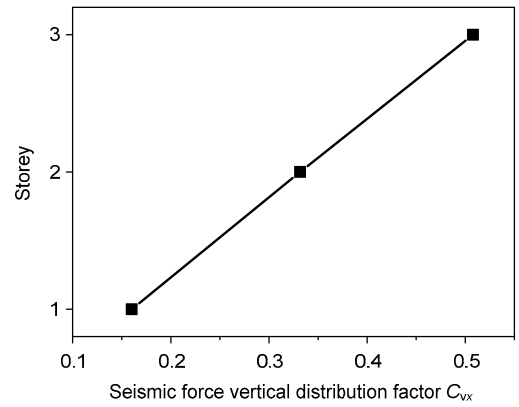

Fig. 18 Vertical distribution factor of seismic force recommended by ASCE/SEI 7-10 (ASCE, 2010)

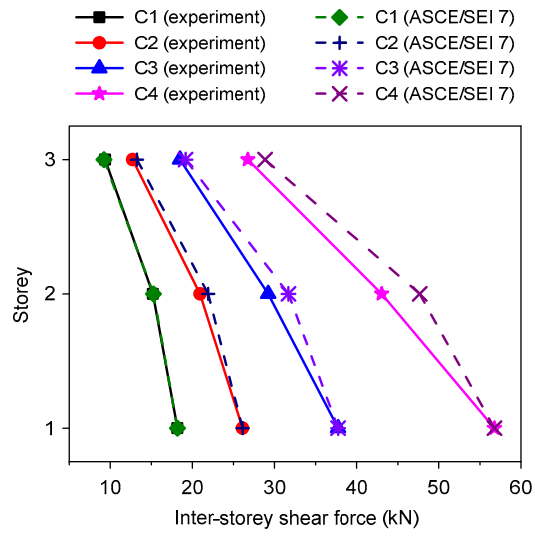

Fig. 19 Maximum inter-storey shear force at each floor

experimentally investigate the seismic performance of the proposed structural system.

The test results showed that beam-only-connected SPSWs buckled at a relatively small inter-storey drift, and post-buckling tension fields were formed to resist lateral loads. With the increase of PGA, diagonal tension fields were further developed and yielded to dissipate earthquake energy. As steel infill panels were connected with only composite beams, no additional tension forces were induced in steel columns, and plastic hinges were initially formed at composite beam ends.

No damage or obvious connector slippage was observed in BHA connections, which was in accordance with the strong connection design principle. The stable force-displacement behavior of the specimen showed that the fabricated composite frame, assembled by BHA connections, exhibited substantial redundancy.

An undesirable failure mode of the fabricated composite frame in huge earthquakes was the horizontal cracks progressed in composite beams and the block shear failure in SPSWs' connections. Owing to the sufficient lateral stiffness provided by beam-only-connected SPSWs, the deformation of the specimen could meet the Chinese seismic design specification requirements. The first storey was the critical position of the prototype building and needed to be well designed to avoid the formation of soft-storeys. The proposed structural system exhibited good energy-dissipating capacity without significant strength and stiffness degradation. The seismic force distribution recommended by ASCE/SEI 7-10 (ASCE, 2010) was validated with experimental data.

References

AISC (American Institute of Steel Construction), 2010. Seismic Provisions for Structural Steel Buildings, ANSI/AISC 341-10. AISC, USA.

ASCE (American Society of Civil Engineers), 2010. Minimum Design Loads for Buildings and Other Structures, ASCE/SEI 7-10. ASCE, USA.

Cao, Z.Z., Du, P., Li, J.D., *et al*., 2015. Research on mechanical performance of bolted height adjustable steel beam-to-column connections under low cycle reversed loading. *Journal of Building Structures*, **36**(4):1-8 (in Chinese). http://dx.doi.org/10.14006/j.jzjgxb.2015.04.001

Clayton, P., Winkley, T., Berman, J., *et al*., 2012a. Experimental investigation of self-centering steel plate

shear walls. *Journal of Structural Engineering*, **138**(7): 952-960. http://dx.doi.org/10.1061/(ASCE)ST.1943-541X.0000531

Clayton, P., Berman, J., Lowes, L., 2012b. Seismic design and performance of self-centering steel plate shear walls. *Journal of Structural Engineering*, **138**(1):22-30. http://dx.doi.org/10.1061/(ASCE)ST.1943-541X.0000421

Dowden, D., Purba, R., Bruneau, M., 2012. Behavior of self-centering steel plate shear walls and design considerations. *Journal of Structural Engineering*, **138**(1):11-21. http://dx.doi.org/10.1061/(ASCE)ST.1943-541X.0000424

Driver, R., Kulak, G., Kennedy, D., *et al*., 1998. Cyclic test of four-storey steel plate shear wall. *Journal of Structural Engineering*, **124**(2):112-120. http://dx.doi.org/10.1061/(ASCE)0733-9445(1998)124:2(112)

Guo, L.H., Rong, Q., Ma, X.B., *et al*., 2011. Behavior of steel plate shear wall connected to frame beams only. *International Journal of Steel Structures*, **11**(4):467-479. http://dx.doi.org/10.1007/s13296-011-4006-7

Kulkarni, S.A., Li, B., Yip, W.K., 2008. Finite element analysis of precast hybrid-steel concrete connections under cyclic loading. *Journal of Constructional Steel Research*, **64**(2):190-201. http://dx.doi.org/10.1016/j.jcsr.2007.05.002

Li, B., Kulkarni, S.A., Leong, C.L., 2009. Seismic performance of precast hybrid-steel concrete connections. *Journal of Earthquake Engineering*, **13**(5):667-689. http://dx.doi.org/10.1080/13632460902837793

Lin, C.H., Tsai, K.C., Qu, B., *et al*., 2010. Sub-structural pseudo-dynamic performance of two full-scale two-storey steel plate shear walls. *Journal of Constructional Steel Research*, **66**(12):1467-1482. http://dx.doi.org/10.1016/j.jcsr.2010.05.013

Liu, C., Wang, Q., Wang, Y., *et al*., 2013. Flexural behavior of precast reinforced concrete beams with steel end connectors. *Journal of Building Structures*, **34**(S1): 208-214 (in Chinese). http://dx.doi.org/10.14006/j.jzjgxb.2013.s1.031

Lubell, A., Prion, H., Ventura, C., *et al*., 2000. Unstiffened steel plate shear wall performance under cyclic loading. *Journal of Structural Engineering*, **126**(4):453-460. http://dx.doi.org/10.1061/(ASCE)0733-9445(2000)126:4(453)

MOHURD (Ministry of Housing and Urban-Rural Development of the People's Republic of China), 1999. Steel and Steel Products—Location and Preparation of Test Pieces for Mechanical Testing, GB/T 2975-1998. MOHURD (in Chinese).

MOHURD (Ministry of Housing and Urban-Rural Development of the People's Republic of China), 2010. Code for Seismic Design of Buildings, GB50011-2010. MOHURD (in Chinese).

MOHURD (Ministry of Housing and Urban-Rural Development of the People's Republic of China), 2011. Metallic Materials-Tensile Testing—Part 1: Method of Test at Room Temperature, GB/T 228.1-2010. MOHURD (in Chinese).

MOHURD (Ministry of Housing and Urban-Rural Development of the People's Republic of China), 2015. Specification for Seismic Test of Buildings, JGJ/T 101-2015. MOHURD (in Chinese).

MOHURD (Ministry of Housing and Urban-Rural Development of the People's Republic of China), 2016. Technical Specification for Steel Plate Shear Walls, JGJ/T 380-2015. MOHURD (in Chinese).

Qu, B., Bruneau, M., Lin, C., *et al*., 2008. Testing of full-scale two-storey steel plate shear wall with reduced beam section connections and composite floors. *Journal of Structural Engineering*, **134**(3):364-373. http://dx.doi.org/10.1061/(ASCE)0733-9445(2008)134:3(364)

Thorburn, L.J., Kulak, G.L., Montgomery, C.J., 1983. Analysis of Steel Plate Shear Walls. Structural Engineering Report No. 107. Department of Civil Engineering, the University of Alberta, Canada. Available from www.civil.ualberta.ca/structures/reports/SER107Thorburn,Kulak,andMontgomery.pdf.

Xue, M., Lu, L.W., 1994. Monotonic and cyclic behavior of infilled steel shear panels. 17th Czech and Slovak International Conference on Steel Structures and Bridges, p.152-160.

Yang, K.H., Oh, M.H., Kim, M.H., *et al*., 2010. Flexural behavior of hybrid precast concrete beams with H-steel beams at both ends. *Engineering Structures*, **32**(9):2940-2949. http://dx.doi.org/10.1016/j.engstruct.2010.05.013

中文概要

题　目： 装配式钢板剪力墙-组合框架结构伪动力试验研究

目　的： 装配式建造技术以其施工速度快和质量可靠等优点而被广泛采用。本文旨在探讨装配式钢板剪力墙-组合框架结构在不同地震烈度下的响应及失效模式，研究该结构体系的抗震性能，评估设计规范 ASCE/SEI 7-10 所推荐地震楼层剪力分布模式的合理性。

创新点： 1. 通过伪动力试验，研究了装配式组合框架结构的抗震性能；2. 分析了两边连接钢板剪力墙应用于装配式结构体系时的受力性能；3. 评估了设计规范 ASCE/SEI 7-10 中地震楼层剪力分布的合理性。

方　法： 1. 通过开展不同地震烈度下的伪动力试验研究，

分析装配式钢板剪力墙-组合框架的地震响应和失效模式；2. 通过对比规范公式与试验数据，验证规范地震楼层剪力分布的合理性。

结　论： 1. 两边连接钢板剪力墙在较小的荷载下屈曲，通过屈曲后形成的拉力带抵抗水平荷载并屈服耗能；2. 由可变梁高装配式钢框架节点拼装而成的装配式组合框架具有稳定的力学性能、良好的耗能能力以及足够的延性；3. 本文所分析的装配式框架试件在大震下发生了组合梁严重开裂以及钢板剪力墙与组合梁之间螺栓连接冲切破坏的现象，应通过合理设计避免该破坏模式；4. 设计规范ASCE/SEI 7-10 所建议的公式可以合理地预测地震楼层剪力分布。

关键词： 装配式框架；组合梁；钢板剪力墙；伪动力试验